

Derivative coupling in horizon brightened acceleration radiation: a quantum optics approach

Ashmita Das^{*} and Anjana Krishnan[†]

Department of Physics, SRM University AP, Amaravati 522240, India

Soham Sen[‡] and Sunandan Gangopadhyay[§]

*Department of Astrophysics and High Energy Physics,
S.N. Bose National Centre for Basic Sciences,
JD Block, Sector III, Salt Lake, Kolkata 700106, India*

Horizon Brightened Acceleration Radiation (HBAR) signifies a unique radiation process and provides a promising framework in exploring acceleration radiation in flat/ curved spacetime. Its construction primarily relies on the transition probability of an atom falling through a high-Q cavity while interacting with a quantum field. The HBAR effect has typically been explored in the context of minimal coupling between the atom and the field amplitude. However, the minimally coupled models are affected by the infrared (IR) divergences that arise in the massless limit of the quantum fields in (1+1) dimensions. Thus, in the present manuscript, we examine the HBAR process using both the point-like and finite size detectors coupled with the momentum of the field, which plays a crucial role in naturally resolving IR divergences. Our results suggest that the transition probability for the point-like detector is independent of its frequency. This can be interpreted as the influence of the local gravitational field which modifies the sensitivity of the detector to its frequency and broadens its effective frequency range. Through a comparative study based on the length of the detector, we find that for a detector with a smaller length, the steady state solution for the density matrix of the field vanishes. This may indicate the existence of a non equilibrium thermodynamic state under the condition of finite size detector-field interaction. These distinctive features are exclusive to the derivative coupling between the atom and the field, highlighting them as a compelling subject for future investigation.

I. INTRODUCTION

An elegant combination of individual disciplines such as general relativity, thermodynamics and quantum field theory (QFT) has brought to us many interesting phenomena. A direct consequence of this fusion is none other than the Hawking radiation from the black hole (BH) spacetime [1, 2], cosmological particle production [3–7], quantum entanglement [8–10], entanglement harvesting [11, 12], relativistic quantum information [13, 14] etc. Moving further the implementation of quantum optics in the studies of acceleration radiation in flat/ curved spacetime provided to us a parallel mechanism to explain the Unruh-Fulling (UF) effect [15]. Using a high-Q microwave cavity, Scully et al. have shown in [15] that ground state atomic detectors when accelerated through the cavity, creates radiation where the transition probability of the detector can be increased to many orders in magnitude than that of the Unruh radiation [16–18]. Furthermore, in 2018 Fulling et al. extended this idea to the BH spacetime and presented a different kind of particle radiation called horizon brightened acceleration radiation (HBAR), unlike the Hawking radiation from the BH [19]. Consequently one obtains the HBAR entropy which has

a different genesis than the Bekenstein-Hawking entropy.

The HBAR phenomenon is based on the virtual processes as we often witness in QFT such as Lamb shift, Raman scattering, etc. Within the atom-field interaction the HBAR phenomenon can be outlined as follows. In the background of a BH spacetime, the two level atomic detectors are freely falling while they traverse through a cavity. The cavity is positioned near the event horizon of the BH such as the Hawking radiated particles can be restricted to enter the cavity. To isolate a single field mode, a mode selector is installed which selects one cavity mode travelling in the opposite direction of the atoms so that the whole set up generates a relative acceleration between the atom and the field mode. This relative acceleration incites the atom to drift away from its original position of virtual emission. This triggers a non-zero probability of not absorbing the emitted virtual photon and transforms a virtual photon into a real one in the final state of the system [15, 19]. Eventually the transition probability, temperature and the entropy associated with the HBAR can be estimated [15, 19]. HBAR scenario has uncovered many notable insights which can be found in the following references [20–28].

The interaction Hamiltonian for the HBAR model can be written as $\sim g\mu(\tau)\Phi(x(\tau))$, where g , $\mu(\tau)$ depict coupling strength and the monopole moment of the atomic detector respectively. $\Phi(x(\tau))$ is the massless scalar field which interacts with the detector and τ represents the proper time of the detector. This minimally coupled model resembles the Hamiltonian of the Unruh-DeWitt

^{*} ashmita.phy@gmail.com

[†] anjana.krishnan@srmmap.edu.in

[‡] sensohomhary@gmail.com, soham.sen@bose.res.in

[§] sunandan.gangopadhyay@gmail.com

(UD) detector interaction with a massless scalar field in the standard UF effect [16, 17].

Identifying this similarity, we turn our focus towards the well known infrared (IR) divergence problem of the standard UF effect for a massless scalar field in $(1+1)$ dimensions. This problem is inbuilt in the Wightman function of a minimally coupled massless field in $(1+1)$ dimensions [29–31]. This IR divergence can be tackled by using a cut-off scale, however, final density matrix and transition probability of the detectors become dependent on the chosen cut-off scale [11, 32, 33]. Subsequently, it was shown that this IR ambiguity can naturally be removed by considering the detector linearly coupled to the proper time derivative of the field amplitude [30–39]. Furthermore the short distance behaviour of derivative coupling in $(1+1)$ dimensions mimics the $(3+1)$ dimensional minimal coupling [32, 39], which leads to the dualities between the derivative and minimally coupled models [40]. Thus, particle detector model with derivative coupling possesses considerable importance in controlling the IR divergence in QFT and offers a simple $(1+1)$ dimensional framework that captures the essential features of minimally coupled particle detector models in $(3+1)$ dimensions, so that complicated treatments of $(3+1)$ dimensions can be avoided. In recent times, several attempts have been taken to study the implications of derivative coupling such as derivative coupling supports the entanglement harvesting when the particle detectors are in causal contact in flat spacetime [38], construction of relativistic communication channel between two localised detectors in arbitrary curved spacetime [41], establishing dualities between minimally coupled particle detector model and derivative coupled model in the limit of large energy gaps [40], etc. Furthermore, using the derivative coupling approach, a UD detector executing uniform circular motion is considered in a $(2+1)$ dimensional background, with the field initially in a thermal state [31]. Obtaining the effective temperature associated with the detector, it was shown in [31] that the effect due to the acceleration radiation can indeed be detected. Under certain conditions, the existence of cooling Unruh effect has also been reported in [31], making the model to be experimentally promising. It is also observed in [42, 43] that the interaction of the atom and derivative of the scalar field captures certain characteristics of the interaction between the atom and electromagnetic field. Derivative coupled models can also be experimentally tested by employing superconducting qubit as a particle detector, coupled to a transmission line which mimics a $(1+1)$ dimensional massless field [44, 45].

Motivated by the implications of derivative coupling, we explore a spontaneous question, what would be the fate of HBAR phenomenon when the atomic detector and the field exhibit derivative coupling? Specifically, we consider a high Q microwave cavity set up in the vicinity of the Schwarzschild BH as described in [19]. The stream of two level atomic detectors are falling freely from infinity towards the BH through the cavity set up. Within

the cavity one or few modes of the quantum matter field can be confined and a mode selector chooses one cavity mode, enabling a relative acceleration between the field mode and the infalling atoms. In this setup, we consider atoms coupled to the momentum of a massless scalar photon, taking into account both point-like and finite size descriptions of the atoms. We summarize our findings below.

- (1) We compute the transition probability of the system up to the first order of perturbation theory for both the point-like and finite size detectors. For the point-like detector, we obtain an enhanced transition probability than as reported in [19]. On the other hand the transition probability for the finite size detector turns out to be dependent on the size of the detector and exhibits suppression for larger extent of the detector.
- (2) For point-like case, we find the temperature of the thermal bath due to the HBAR to be $T = \frac{\hbar c^3}{8\pi G M_{\text{BH}} k_B}$, where \hbar , c , and k_B represent reduced Planck's constant, speed of light in vacuum and the Boltzmann constant respectively. G is the Newton's gravitational constant and M_{BH} depict the mass of the Schwarzschild BH. For the finite size detector two conditions emerge such as $L\omega \gtrsim 1$ and $L\omega \lesssim 1$, where L represents the length of the detector and ω stands for the frequency of the same. Physically we interpret these conditions as larger and smaller length detectors for a fixed frequency ω . Thus, for $L\omega \gtrsim 1$, we obtain a well defined temperature of the thermal bath, similar to the point-like case whereas for $L\omega \lesssim 1$, the transition probability displays non-Planckian characteristics, indicating that no well defined temperature can be assigned.
- (3) We find the microscopic change in the density matrix of the field due to the radiation and subsequently derive the steady state solution for the same. In case of the point-like detector, the steady state solution remains same as in [19]. For the finite size detector, under the condition $L\omega \gtrsim 1$, the steady solution is obtained, however, it becomes zero for $L\omega \lesssim 1$.
- (4) In this framework, the entropy associated to HBAR exhibits a similar area entropy relation as one obtains for the standard BH solutions and in [19].
- (5) We implement the phenomenon of Wien displacement and make a comparative study between the wavelengths of the emitted radiation, which correspond to the maximum transition probability in both the minimal and derivative coupled models. In case of point-like and finite size detector with the condition $L\omega \gtrsim 1$, the nature of the λ vs. temperature plot exhibit the same pattern.

The inclusion of derivative coupling between the atom and the field leads to modified behaviours that not only resolve the IR divergence problem found in the minimally coupled model but also introduce unique characteristics in the HBAR phenomenon.

The present manuscript is organised as follows. In the upcoming section (II), we describe the trajectory of the atomic detector and write the field equations in the background of Schwarzschild spacetime. Sections (III) and (IV) discuss the interaction of point-like and finite size detectors with the momentum of a massless scalar photon and derive the corresponding excitation probabilities, the density matrix of the field, steady state solution and area-entropy law. In section (V), relating to the Wien's displacement law, we examine how the radiation wavelength varies with respect to the temperature of the bath and present a comparative study between the amplitude and derivative coupled models.

II. TRAJECTORY OF THE ATOMIC DETECTOR AND MODE SOLUTION FOR THE FIELD IN THE BACKGROUND OF SCHWARZSCHILD SPACETIME

In this section, we review the trajectory of a freely falling atomic detector in the background of a Schwarzschild BH where we consider the $t - r$ part of the metric as follows [19],

$$ds^2 = \left(1 - \frac{r_g}{r}\right) - \left(1 - \frac{r_g}{r}\right)^{-1} dr^2, \quad (1)$$

where $r_g = \frac{2GM_{BH}}{c^2}$ is the radius of the event horizon of the BH. At this stage we introduce a dimensionless coordinate where $r_g, r_g/c$ are treated as the unit of the distance and time respectively. Therefore, following [19] we write.

$$r \rightarrow r_g r, \quad t \rightarrow (r_g/c) t, \quad \omega \rightarrow (c/r_g). \quad (2)$$

Note that in the transformation the parameters at the right hand side of the arrow head represent dimensionless parameters. In terms of dimensionless Schwarzschild coordinates, the trajectory of the infalling atom with respect to its dimensionless proper time τ becomes,

$$\frac{dr}{d\tau} = -\frac{1}{\sqrt{r}}, \quad \frac{dt}{d\tau} = \frac{r}{r-1}. \quad (3)$$

Solving these equations one obtains,

$$\tau = -\frac{2}{3}r^{3/2} + \text{const.} \quad (4)$$

$$t = -\frac{2}{3}r^{3/2} - 2\sqrt{r} - \ln\left(\frac{\sqrt{r}-1}{\sqrt{r}+1}\right) + \text{const.} \quad (5)$$

At this stage, we follow the procedure developed in [15, 19] and consider the Klein Gordon equation for a massless scalar photon with wave function ϕ as,

$$\frac{1}{\sqrt{-g}}\partial_\mu(\sqrt{-g}g^{\mu\nu}\partial_\nu)\phi = 0. \quad (6)$$

Imposing the s-wave approximation and a coordinate transformation $r_* = r + \ln(r-1)$, in the above equation one obtains,

$$\left(\frac{\partial^2}{\partial t^2} - \frac{\partial^2}{\partial r_*^2}\right)\phi = 0 \quad (7)$$

The solution of the Eq. (7) turns out to be,

$$\phi = e^{i\nu(t-r_*)} = e^{i\nu[t-r-\ln(r-1)]}, \quad (8)$$

where, ν depicts the frequency of the photon field. In the upcoming section we turn our focus to explore the HBAR phenomenon in case of the point-like detector interacting with the momentum of a massless scalar photon.

III. HBAR FOR THE POINT-LIKE DETECTOR COUPLED TO THE MOMENTUM OF THE FIELD IN THE BACKGROUND OF SCHWARZSCHILD BH

We write the interaction Hamiltonian of a point-like detector with the momentum of a massless scalar photon as follows [18],

$$H_{int} = \hbar g \mu(\tau) \sqrt{-g} g^{00} \partial_0 \left(a_\nu e^{-i\nu t(\tau) + i\nu r_*(\tau)} + \text{H.C.} \right) \quad (9)$$

where g is the coupling constant and $\mu(\tau) = \sigma e^{-i\omega\tau} + \sigma^\dagger e^{i\omega\tau}$ is the monopole moment operator of the detector. The momentum of the field in the curved spacetime can be defined as, $\pi(\tau) = \sqrt{-g} g^{00} [\partial_0 \Phi(\tau)]$ [18]. Here $\Phi(\tau) = (a_\nu e^{-i\nu t(\tau) + i\nu r_*(\tau)} + \text{H.C.})$, represents the massless scalar field. g_{00} denotes the zeroth component of the $(3+1)$ dimensional Schwarzschild metric and $\sqrt{-g}$ is the determinant of the metric tensor $g_{\mu\nu}$. In the dimensionless Schwarzschild coordinates g^{00} becomes $\frac{r}{r-1}$. $\sqrt{-g} = r^2 \sin\theta$, which simplifies to $\sqrt{-g} = r^2$ when restricted to the equatorial plane, *i.e.*, at $\theta = \frac{\pi}{2}$. The initial and the final state of the system can be represented as, $|0, a\rangle$ and $|1_\nu, b\rangle$ respectively, where $(0, 1_\nu)$ are the vacuum and 1-particle state of the matter field with a particular frequency ν and (a, b) depict the ground and excited state of the detector. At this stage we refer our readers to [19] for an elaborate review of this set up. Therefore, decomposing the field operator and operating the time derivative on the field modes we obtain,

$$H_{int} = i \hbar g \nu \mu(\tau) \frac{r^3}{r-1} \left(a_\nu^\dagger e^{i\nu(t-r_*)} - a_\nu e^{-i\nu(t-r_*)} \right). \quad (10)$$

Using Eqs. (4), (5) and $r_* = r_*(r)$, the transition probability is found to be,

$$P_{exc} = \frac{1}{\hbar^2} \left| \int d\tau \langle 1, b | H_{int} | 0, a \rangle \right|^2 = g^2 \nu^2$$

$$\left| \int_1^{r'} dr \left(\frac{r^{7/2}}{r-1} \right) e^{-i\nu(\frac{2}{3}r^{3/2} + r + 2\ln(r^{1/2}-1) + 2r^{1/2})} e^{-\frac{2i\omega}{3}r^{3/2}} \right|^2 \quad (11)$$

where r' is considered to be $1 \lesssim r' < 2$, depicting the near horizon region of the BH. Note from the previous discussion that, in the dimensionless Schwarzschild coordinates, the radius of the event horizon turns out to be 1. Substituting $y = r^{3/2}$ in Eq. (11), we find,

$$P_{exc} = \frac{4g^2\nu^2}{9} \left| \int_1^{y'} dy \left(\frac{y^2}{y^{2/3}-1} \right) e^{-i\nu(\frac{2}{3}y + y^{2/3} + 2y^{1/3} + 2\ln(y^{1/3}-1))} e^{-\frac{2i\omega}{3}y} \right|^2, \quad (12)$$

where $y' = r'^{3/2}$ is the upper limit of integration. Since we are still working in the near horizon regime, we restrict y' to the range $1 \lesssim y' < 2$. Substituting $x = \frac{2\omega}{3}(y-1)$ one obtains $x < \frac{2\omega}{3}$ and thus the above equation can be recast as follows,

$$P_{exc} = \frac{g^2\nu^2}{\omega^2} \left| \int_0^{x'} dx \left(\frac{\omega}{x} + 3 \right) e^{-ix(1+\frac{2\nu}{\omega})} x^{-2i\nu} \right|^2. \quad (13)$$

where $x' = \frac{2\omega}{3}(y'-1)$. It is important to note that $x < \frac{2\omega}{3} \implies \frac{x}{\omega} < \frac{2}{3} < 1$. Some important observations are now in order. The functions $x^{-2i\nu}$ and $e^{-ix(1+\frac{2\nu}{\omega})}$ are both oscillatory in nature. In Fig.(1),

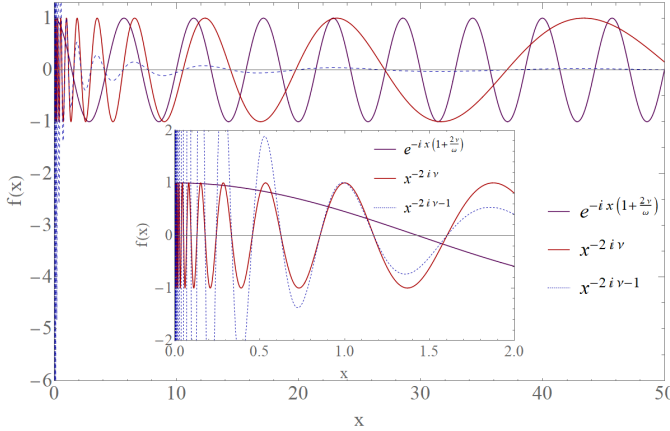


FIG. 1: Real part of the functions $f(x) = \{e^{-ix(1+\frac{2\nu}{\omega})}, x^{-2i\nu}, x^{-2i\nu-1}\}$ are plotted against x for $\frac{\nu}{\omega} = \frac{1}{20}$.

we plot the real part of the following functions $f(x) = \{e^{-ix(1+\frac{2\nu}{\omega})}, x^{-2i\nu}, x^{-2i\nu-1}\}$ with respect to x , while keeping $\nu = 5$ and $\omega = 100$ fixed in the dimensionless unit. From Fig.(1), it can be perceived that in the large x limit $x^{-2i\nu}$ varies slowly with respect to the oscillatory $e^{-ix(1+\frac{2\nu}{\omega})}$ function and the effect of the $x^{-1-2i\nu}$ almost dies out. Conversely, we observe from the inset

plot that, for small x regime the exponential function is slowly varying in comparison to $x^{-2i\nu}$ as well as $x^{-2i\nu-1}$. This functional behaviour of $x^{-2i\nu}$ is also known as the ‘‘Russian doll behaviour’’ [21]. As a result, the dominant contribution to the integral in eq.(13), shall come from the regime where $0 \leq \frac{x}{\omega} \lesssim 1$. On the other hand, in large x regime, due to the highly oscillatory nature of the exponential function compared to the $x^{-2i\nu}$, the overall contributions to the integral can be neglected. As a result, it is possible to extend the upper limit of integration from x' to ∞ without affecting the analysis. This recasts Eq.(13) in the following form,

$$P_{exc} = \frac{g^2\nu^2}{\omega^2} \left| \int_0^\infty dx \left(\frac{\omega}{x} + 3 \right) e^{-ix(1+\frac{2\nu}{\omega})} x^{-2i\nu} \right|^2. \quad (14)$$

Using $u = x(1 + \frac{2\nu}{\omega})$ and performing the integral, the transition probability turns out to be,

$$P_{exc} = \frac{g^2\nu^2}{\omega^2} \left| \Gamma(-2i\nu) e^{-\pi\nu} (\omega - 4\nu) \right|^2 = \frac{g^2\nu\pi}{(1 + \frac{2\nu}{\omega})^2} \left(1 - \frac{4\nu}{\omega} \right)^2 \frac{1}{e^{4\pi\nu} - 1}, \quad (15)$$

where we use the identity $\Gamma(ix) = \frac{\pi}{x \sinh(\pi x)}$. It is apparent that for $\nu \gg 1$, the transition probability is exponentially suppressed. For characteristic atomic frequencies, $\omega \gg 1$, therefore, it is reasonable to focus on the domain where, in general $\nu \ll \omega$. Under this condition the transition probability emerges as,

$$P_{exc} = g^2\nu \left(\frac{1}{e^{4\pi\nu} - 1} \right). \quad (16)$$

In dimensionful units, Eq. (16) can be recast as,

$$P_{exc} = \frac{g^2\nu r_g \pi}{c} \frac{1}{e^{4\pi\nu r_g/c} - 1}. \quad (17)$$

Subsequently, we obtain the absorption probability by altering $\nu \rightarrow -\nu$, which yields the absorption probability (P_{abs}) as below,

$$P_{abs} = e^{4\pi\nu r_g/c} P_{exc}. \quad (18)$$

Eq. (17) demonstrates that the transition probability of the system under the leading order approximation of the time dependent perturbation theory, becomes independent of the detector’s frequency. We propose that momentum coupling in curved spacetime explicitly introduces a connection between the spacetime curvature, *i.e.*, the gravitational field, and the detector. This interaction may provide enough energy to the detector to assist its transition without the need for exact resonance at a particular frequency. Consequently, the resulting transition probability becomes independent of the detector’s frequency [32]. We illustrate how the transition probability

varies with the field frequency and provide a comparative analysis of P_{exc} as derived from both the minimally coupled model [19] and the momentum coupled model. For the purpose of the plotting, we treat all the parameters in dimensionless unit.

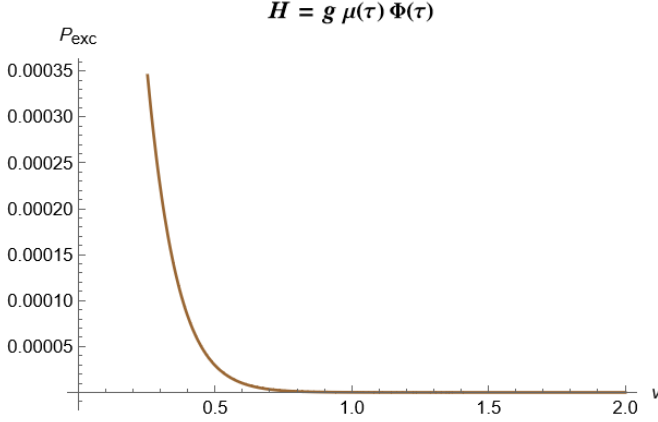


FIG. 2: P_{exc} vs ν plot for minimal coupling between the detector and the field. g is set to be 1 while $\omega = 20$

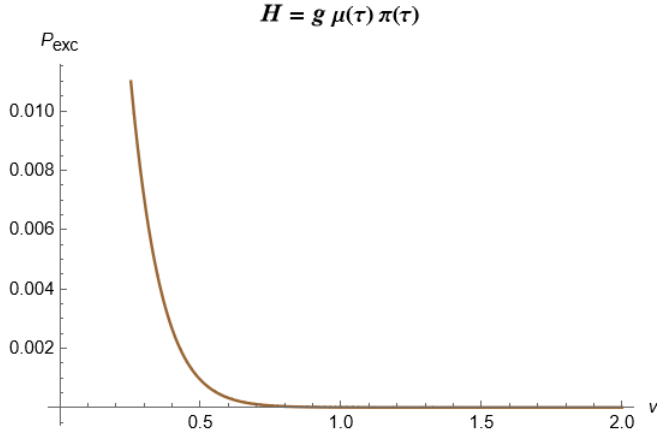


FIG. 3: P_{exc} vs ν plot for the detector coupled with the momentum of the field. g is set to be 1

A. Density matrix for the field mode and HBAR entropy: point-like case

In this section, we find the entropy flux corresponding to the HBAR in case of the point-like detector interacting with the momentum of the field. Following the treatment from quantum optics as used in [15, 19, 23], we first write the microscopic change in the field density matrix as, $\delta\rho_i$ due to a single atom-field interaction. Consequently, the macroscopic change in the same due to the $\Delta\mathcal{N}$ number of atoms can be written as [15, 19, 23],

$$\Delta\rho = \sum_i \delta\rho_i = \Delta\mathcal{N} \delta\rho = \kappa \Delta t \delta\rho \quad (19)$$

$$\Rightarrow \frac{\Delta\rho}{\Delta t} = \kappa \delta\rho. \quad (20)$$

Here, κ denotes the rate at which the atoms fall into the event horizon of the BH. Using the Lindblad master equation for the density matrix one obtains,

$$\begin{aligned} \dot{\rho}_{n,n} = & -R_a [n\rho_{n,n} - (n+1)\rho_{n+1,n+1}] \\ & -R_e [(n+1)\rho_{n,n} - n\rho_{n-1,n-1}], \end{aligned} \quad (21)$$

where, R_e, R_a symbolize emission and absorption rates of the photons in the cavity by the atom and these rates are defined as, $R_{e/a} = \kappa P_{exc/abs}$. Thus, in terms of the excitation and absorption rates, the steady state solution becomes,

$$\rho_{n,n}^S = \left(\frac{R_e}{R_a}\right)^n \left(1 - \frac{R_e}{R_a}\right). \quad (22)$$

Using Eqs.(17) and (18), the steady state solution for the density matrix of the field turns out to be,

$$\begin{aligned} \rho_{n,n}^S &= \left(\frac{P_{exc}}{P_{abs}}\right)^n \left(1 - \frac{P_{exc}}{P_{abs}}\right) \\ &= e^{-4\pi\nu nr_g/c} (1 - e^{-4\pi\nu r_g/c}). \end{aligned} \quad (23)$$

Furthermore, using the density matrix of the field we aim to find the Von Neumann entropy for the system. Thus, the time rate of change of entropy within the cavity due to the photon emission becomes,

$$\dot{S}_p = -k_B \sum_{n,\nu} \dot{\rho}_{n,n} \ln(\rho_{n,n}). \quad (24)$$

Using the steady state solution of the density matrix, the above equation can approximately be written as,

$$\dot{S}_p \approx -k_B \sum_{n,\nu} \dot{\rho}_{n,n} \ln(\rho_{n,n}^S). \quad (25)$$

Subsequently, using Eq. (23) in Eq. (24) we obtain,

$$\begin{aligned} \dot{S}_p &= -k_B \sum_{n,\nu} \dot{\rho}_{n,n} \left[\frac{-4\pi\nu nr_g}{c} + \ln(1 - e^{-4\pi\nu r_g/c}) \right] \\ &\approx k_B \sum_{n,\nu} \dot{\rho}_{n,n} \frac{4\pi\nu nr_g}{c} = k_B \frac{4\pi r_g}{c} \sum_{\nu} \dot{\eta}_{\nu} \nu. \end{aligned} \quad (26)$$

Here, $\dot{\eta}_{\nu} = \sum_n n \dot{\rho}_{n,n}$ depicts flux of the produced photons in the cavity.

The area of the BH can be written as $A_{BH} = 4\pi r_g^2 = \frac{16\pi G^2 M_{BH}^2}{c^4}$, and we write the rate of change of the rest mass of the BH as below,

$$\dot{M}_{BH} = \dot{M}_{photon} + \dot{M}_{atom}, \quad (27)$$

where \dot{M}_{atom} represents the rate of change of mass of the BH due to the injection of the atomic cloud, and \dot{M}_{photon} depicts rate of change of mass of the BH due to the extraction of energy by the emitted photons from the

rest mass energy of the BH. Differentiating the area of the BH with respect to time we obtain,

$$\dot{A}_{\text{BH}} = \frac{32\pi G^2 M_{\text{BH}} \dot{M}_{\text{BH}}}{c^4}. \quad (28)$$

Using the above equation and area of BH we write,

$$\dot{A}_{\text{BH}} = \frac{2 \dot{M}_{\text{BH}} A_{\text{BH}}}{M_{\text{BH}}} = \frac{2 A_{\text{BH}} (\dot{M}_{\text{photon}} + \dot{M}_{\text{atom}})}{M_{\text{BH}}}. \quad (29)$$

Eq. (29) can also be expressed as follows,

$$\dot{A}_{\text{BH}} = \dot{A}_{\text{photon}} + \dot{A}_{\text{atom}}, \quad (30)$$

which, upon comparison with Eq. (29), implies

$$\begin{aligned} \dot{A}_{\text{photon(atom)}} &= \frac{2 A_{\text{BH}} \dot{M}_{\text{photon(atom)}}}{M_{\text{BH}}} \\ &= \frac{32\pi G^2 M_{\text{BH}} \dot{M}_{\text{photon(atom)}}}{c^4}. \end{aligned} \quad (31)$$

Eq. (30) indicates that the rate of change of the area of the BH is a summation of the rate of change of the area due to the photon emission and injection of atomic cloud near the BH. At this stage, we focus on the rate of change of entropy of the BH, only due to the photon emission and write,

$$\dot{S}_p = k_B \frac{4\pi r_g}{c\hbar} \sum_{\nu} \hbar \dot{n}_{\nu} \nu = k_B \frac{4\pi r_g}{c\hbar} \dot{M}_{\text{photon}} c^2, \quad (32)$$

where, using Eq. (31) and $r_g = \frac{2GM_{\text{BH}}}{c^2}$, we arrive at the following expression,

$$\dot{S}_p = \frac{k_B c^3}{4\hbar G} \dot{A}_{\text{photon}}. \quad (33)$$

Eq. (33) demonstrates the relation between the rate of change of HBAR entropy due to the emission of the photon and the area of the BH. For the detailed derivation of the density matrix we refer our readers to the Appendix (VIB).

IV. HBAR FOR THE FINITE SIZE DETECTOR COUPLED TO THE MOMENTUM OF THE FIELD IN THE BACKGROUND OF SCHWARZSCHILD BH

In this section, we consider the interaction where a finite size detector is coupled to the momentum of the scalar photon in the Schwarzschild BH spacetime. We explore the implications of finite size detector, as in reality, any kind of detectors possess spatial extension. In addition, a point-like detector interacting with fields suffers from the ultraviolet (UV) divergences due to the singularity that appear in the field correlation functions at coincidence limit [46–50]. To resolve the UV ambiguity in case of the point-like detector, several regularization

schemes are introduced. For the regularisation schemes, we refer our readers to [46] and the references therein. We write the interaction Hamiltonian for the finite size detector as follows,

$$\begin{aligned} H_{\text{int}} &= \hbar g (\sigma e^{-i\omega\tau} + \sigma^\dagger e^{i\omega\tau}) \int dr' F(r') \sqrt{-g} g^{00} \partial_0 \phi \\ &= i \hbar g \nu (\sigma e^{-i\omega\tau} + \sigma^\dagger e^{i\omega\tau}) \int dr' F(r') \frac{r^3}{r-1} \\ &\quad \left(a_\nu^\dagger e^{i\nu(t-r_*)} - a_\nu e^{-i\nu(t-r_*)} \right) \end{aligned} \quad (34)$$

Here g represents the coupling strength of the finite size detector with the field and $F(r)$ is the smearing function of the detector having a gaussian structure given by [49],

$$F(r) = \frac{\exp[-(r-1)^2/2L^2]}{L\sqrt{2\pi}}. \quad (35)$$

In the figure (4), we present a schematic illustrating a finite size detector falling radially towards the Schwarzschild BH, maintaining the horizontal orientation. For simplicity, we consider the detector to be oriented horizontally, so that complications arising from changes in the detector's proper time due to the gravitational effects of the BH can be avoided. The finite size detector is coupled with the momentum of a massless scalar photon. The length of the detector is so small that we have ignored any kind of tidal effects in the detector arm.

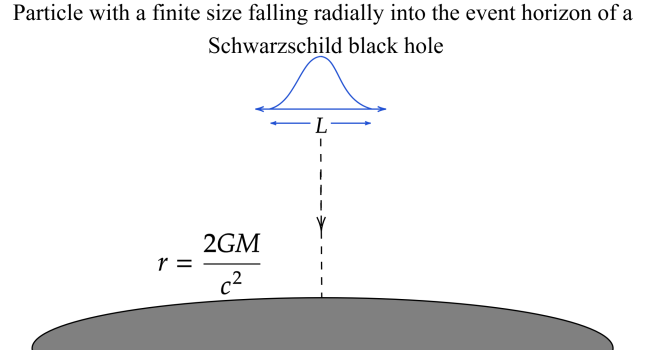


FIG. 4

Following the similar approach as followed in case of the point-like detector, we write,

$$\begin{aligned} P_{\text{exc}} &= \frac{16g^2\nu^2}{162\pi L^2} \left| \int_1^\infty dy e^{-\frac{2i\omega}{3}y} \int_1^y dy' \left(\frac{y'^{5/3}}{y'^{2/3}-1} \right) \right. \\ &\quad \left. e^{-\frac{(y'^{2/3}-1)^2}{2L^2}} e^{-i\nu(\frac{2}{3}y'+y'^{2/3}+2y'^{1/3}+2\ln(y'^{1/3}-1))} \right|^2 \end{aligned} \quad (36)$$

where, we substitute $y = r^{3/2}$. Subsequently we replace $x = \frac{2\omega}{3}(y-1)$ and treat the transformation of $y' \rightarrow x'$ in a similar manner. Thus, the transition probability turns out to be,

$$P_{\text{exc}} = \frac{g^2\nu^2}{32\pi L^2\omega^2} \left| \int_0^\infty dx e^{-ix} e^{-x^2/2\omega^2 L^2} x^{-2i\nu} \left[\frac{5i}{\nu} e^{-2ix\nu/\omega} \right] \right|^2$$

$$+6 \operatorname{EI} \left(1 + 2i\nu, \frac{2i\nu x}{\omega} \right) - 6 \left(\frac{2i\nu x}{\omega} \right)^{2i\nu} \Gamma(-2i\nu) \Big] \Big|^2. \quad (37)$$

Further, using trigonometric hyperbolic identities and gamma function identities given below,

Here, EI represents exponential integral, and expanding the function up to the leading order of x/ω we find [19],

$$\begin{aligned} \operatorname{EI} \left(1 + 2i\nu, \frac{2i\nu x}{\omega} \right) &= \left(\frac{2i\nu x}{\omega} \right)^{2i\nu} \Gamma(-2i\nu) \\ \exp \left[-4\pi\nu \operatorname{Floor} \left(\frac{\pi - \operatorname{Arg}(x/\omega) - \operatorname{Arg}(i\nu)}{2\pi} \right) \right] &+ \frac{-i}{2\nu} \\ &- \frac{2\nu x}{\omega(i+2\nu)}. \end{aligned} \quad (38)$$

As we are in the very near horizon regime, x is small, and any residual effects in the large x limit gets suppressed by the exponential decay factor. At the same time, as ω is large, it is legitimate to adopt the $\frac{x}{\omega} < 1$ approximation in the following analysis. Now, the floor function in the above expression can be expressed as,

$$\begin{aligned} \operatorname{Floor} \left(\frac{\pi - \operatorname{Arg}(x/\omega) - \operatorname{Arg}(i\nu)}{2\pi} \right) &= \operatorname{Floor} \left(\frac{\pi - 0 - \pi/2}{2\pi} \right) \\ &= \operatorname{Floor} \left(\frac{\pi/2}{2\pi} \right) = \operatorname{Floor} \left(\frac{1}{4} \right) = 0. \end{aligned}$$

Substituting the floor function from Eq. (39) into Eq. (38), one obtains,

$$\begin{aligned} \operatorname{EI} \left(1 + 2i\nu, \frac{2i\nu x}{\omega} \right) &= \left(\frac{2i\nu x}{\omega} \right)^{2i\nu} \Gamma(-2i\nu) \\ &+ \frac{-i}{2\nu} - \frac{2\nu x}{\omega(i+2\nu)}. \end{aligned} \quad (40)$$

Using Eq. (40), and implementing $\nu/\omega \ll 1$, the transition probability as in Eq. (37), becomes,

$$P_{exc} = \frac{g^2}{32\pi L^2 \omega^2} \left| \frac{2L^2 \omega^2}{1+2\nu} (i+2\nu) {}_1F_1 \left(1-i\nu, \frac{3}{2}, \frac{-L^2 \omega^2}{2} \right) \right|$$

$$\begin{aligned} &\Gamma(1-i\nu) + 2\sqrt{2}iL\omega\Gamma\left(\frac{1}{2}-i\nu\right) {}_1F_1\left(\frac{1}{2}-i\nu, \frac{1}{2}, \frac{-L^2 \omega^2}{2}\right) \Big|^2. \quad (41) \\ &P_{exc} = \frac{g^2}{8\pi} \left[\left| \nu L\omega\Gamma(-i\nu) \left(1 - \frac{(1-i\nu)L^2 \omega^2}{3} \right) \right|^2 + \right. \\ &\left. \left| \frac{1}{\sqrt{2}}\Gamma\left(\frac{1}{2}-i\nu\right) \left(1 - \left(\frac{1}{2}-i\nu\right)L^2 \omega^2 \right) \right|^2 - \frac{\nu L\omega}{\sqrt{2}} \right. \\ &\left. \left\{ \Gamma\left(\frac{1}{2}-i\nu\right)\Gamma(i\nu) \left(1 - \frac{(1+i\nu)L^2 \omega^2}{3} \right) \right. \right. \\ &\left. \left(1 - (1-2i\nu)\frac{L^2 \omega^2}{2} \right) + \Gamma\left(\frac{1}{2}+i\nu\right)\Gamma(-i\nu) \right. \\ &\left. \left. \left(1 - \frac{(1-i\nu)L^2 \omega^2}{3} \right) \left(1 - (1+2i\nu)\frac{L^2 \omega^2}{2} \right) \right\} \right]. \quad (48) \end{aligned}$$

At this stage, we refer our readers to the Appendix (VI A) for the detailed derivation of this section.

Notably, the confluent hypergeometric function has argument $L^2 \omega^2/2$. Thus, we study both the argument $L\omega/\sqrt{2} > 1$ and $L\omega/\sqrt{2} < 1$. For $L\omega/\sqrt{2} > 1$, the confluent hypergeometric function can be expanded as follows,

$${}_1F_1(a, b, -z) \approx \Gamma(b) \frac{-z^{-a}}{\Gamma(b-a)}, \quad (42)$$

which yields the transition probability as below,

$$P_{exc} = \frac{g^2}{32\pi L^2 \omega^2} \left| 2\sqrt{\pi} \left[\frac{\Gamma(1-i\nu)}{\Gamma(\frac{1}{2}-i\nu)} + i \frac{\Gamma(\frac{1}{2}-i\nu)}{\Gamma(i\nu)} \right] \right|^2 \quad (43)$$

the final form of the transition probability becomes,

$$P_{exc} = \frac{g^2 \nu}{2L^2 \omega^2} \left(\frac{1}{e^{4\pi\nu} - 1} \right) = \frac{g^2 \nu r_g c}{2L^2 \omega^2} \left(\frac{1}{e^{4\pi\nu r_g/c} - 1} \right).$$

Following section (III), the absorption probability turns out to be,

$$P_{abs} = e^{4\pi\nu r_g/c} P_{exc}. \quad (45)$$

For the other condition $L\omega/\sqrt{2} < 1$, the confluent hypergeometric function in Eq. (41), can be expanded as follows,

$${}_1F_1(a, b, z) = \sum_0^\infty \frac{a^n z^n}{b^n n!}. \quad (46)$$

Using Eq. (46), the transition probability becomes,

$$\begin{aligned} P_{exc} &= \frac{g^2}{32\pi L^2 \omega^2} \left| 2L^2 \omega^2 \Gamma(1-i\nu) \left(1 - \frac{(1-i\nu)L^2 \omega^2}{3} \right) \right. \\ &+ \frac{2iL\omega}{\sqrt{2}} \Gamma\left(\frac{1}{2}-i\nu\right) \left(1 - \left(\frac{1}{2}-i\nu\right)L^2 \omega^2 \right) \Big|^2. \end{aligned} \quad (47)$$

Eq. (47) further reduces to,

$$\begin{aligned} &\left| \nu L\omega\Gamma(-i\nu) \left(1 - \frac{(1-i\nu)L^2 \omega^2}{3} \right) \right|^2 + \\ &\left| \frac{1}{\sqrt{2}}\Gamma\left(\frac{1}{2}-i\nu\right) \left(1 - \left(\frac{1}{2}-i\nu\right)L^2 \omega^2 \right) \right|^2 - \frac{\nu L\omega}{\sqrt{2}} \\ &\left\{ \Gamma\left(\frac{1}{2}-i\nu\right)\Gamma(i\nu) \left(1 - \frac{(1+i\nu)L^2 \omega^2}{3} \right) \right. \\ &\left(1 - (1-2i\nu)\frac{L^2 \omega^2}{2} \right) + \Gamma\left(\frac{1}{2}+i\nu\right)\Gamma(-i\nu) \\ &\left. \left(1 - \frac{(1-i\nu)L^2 \omega^2}{3} \right) \left(1 - (1+2i\nu)\frac{L^2 \omega^2}{2} \right) \right\}. \quad (48) \end{aligned}$$

Writing the Gamma functions in the polar form as below,

$$\left. \begin{aligned} \Gamma(z) &= |\Gamma(z)| e^{i \arg \Gamma(z)} \\ \arg \Gamma(z) &= -\arg \Gamma(z^*) \end{aligned} \right\}, \quad (49)$$

and using Eqs. (49) and (44), we have

$$\left\{ \begin{array}{l} \Gamma\left(\frac{1}{2} + i\nu\right) = \sqrt{\frac{\pi}{\cosh \pi\nu}} e^{-i \arg \Gamma(\frac{1}{2} - i\nu)} \\ \Gamma\left(\frac{1}{2} - i\nu\right) = \sqrt{\frac{\pi}{\cosh \pi\nu}} e^{i \arg \Gamma(\frac{1}{2} - i\nu)} \\ \Gamma(i\nu) = \sqrt{\frac{\pi}{\nu \sinh \pi\nu}} e^{-i \arg \Gamma(-i\nu)} \\ \Gamma(-i\nu) = \sqrt{\frac{\pi}{\nu \sinh \pi\nu}} e^{i \arg \Gamma(-i\nu)} \end{array} \right. \quad (50)$$

Thus, the excitation probability turns out to be,

$$P_{exc} = \frac{g^2}{8} \left[\frac{1}{2 \cosh \pi\nu} \left(1 - \frac{L^2 \omega^2}{2} + i\nu L^2 \omega^2 \right)^2 + \frac{L^2 \omega^2 \nu}{\sinh \pi\nu} \left(1 - \frac{L^2 \omega^2}{3} + \frac{i\nu L^2 \omega^2}{3} \right)^2 - \frac{\nu L \omega}{\sqrt{\nu \sinh 2\pi\nu}} \left\{ \left(1 - \frac{5\omega^2 L^2}{6} + \frac{2i\nu L^2 \omega^2}{3} \right) e^{i\chi} + \left(1 - \frac{5\omega^2 L^2}{6} - \frac{2i\nu L^2 \omega^2}{3} \right) e^{-i\chi} \right\} \right], \quad (51)$$

where $\chi = \arg \Gamma(\frac{1}{2} - i\nu) - \arg \Gamma(-i\nu)$. As $L\omega/\sqrt{2} < 1$, we keep the terms up to the $\mathcal{O}(L\omega/\sqrt{2})^2$ in the final form of the transition probability which emerges as,

$$P_{exc} \approx \frac{g^2}{8} \left[\frac{1 - L^2 \omega^2}{e^{\pi\nu} + e^{-\pi\nu}} + \frac{2\nu L^2 \omega^2}{e^{\pi\nu} - e^{-\pi\nu}} - \frac{L\omega\sqrt{2\nu}}{\sqrt{e^{2\pi\nu} - e^{-2\pi\nu}}} \left\{ 2 \left(1 - \frac{5\omega^2 L^2}{6} \right) \cos \chi - \frac{4\nu L^2 \omega^2}{3} \sin \chi \right\} \right]. \quad (52)$$

We obtain the absorption probability to be $P_{abs} = P_{exc}$ under the condition $L\omega/\sqrt{2} < 1$.

At this stage, we examine how P_{exc} varies with the field frequency while keeping $L\omega/\sqrt{2}$ fixed in both the regimes, $L\omega/\sqrt{2} < 1$ and $L\omega/\sqrt{2} > 1$. We identify the

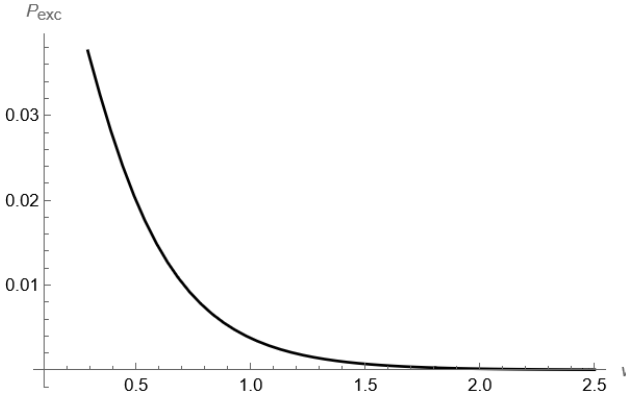


FIG. 5: P_{exc} vs ν plot for finite size detector under the condition $L\omega/\sqrt{2} < 1$.

enhanced transition probability amplitude in Fig. (5) than that of the Fig. (6). Subsequently, in Figures (7) and (8), we plot P_{exc} with respect to $L\omega$ considering both the conditions $L\omega/\sqrt{2} < 1$ and $L\omega/\sqrt{2} > 1$, with the constant field frequencies.

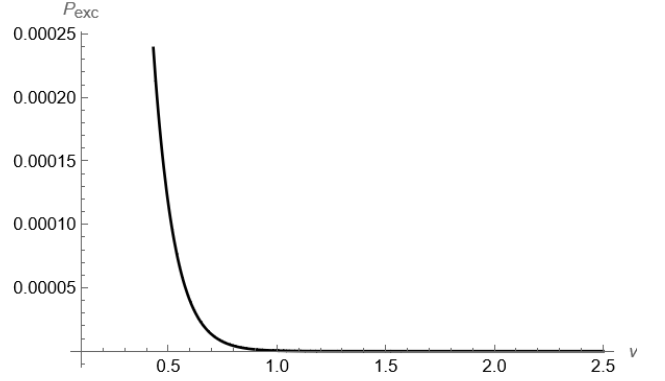


FIG. 6: P_{exc} vs ν plot for finite size detector under the condition $L\omega/\sqrt{2} > 1$.

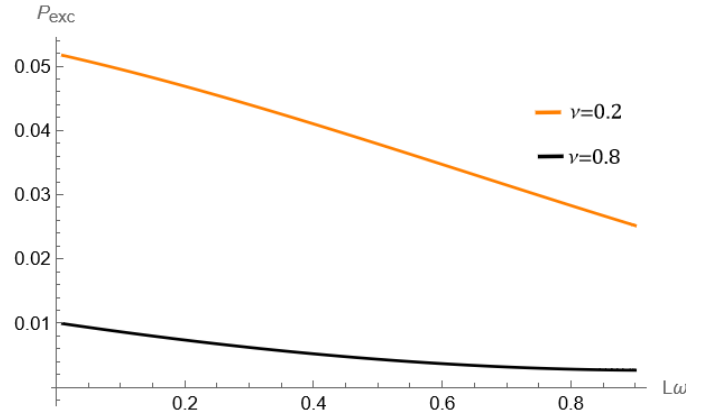


FIG. 7: P_{exc} vs $L\omega$ plot for finite size detector under the condition $L\omega/\sqrt{2} < 1$.

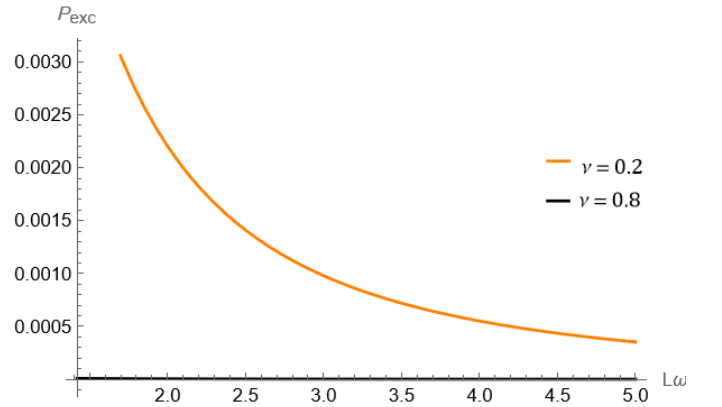


FIG. 8: P_{exc} vs $L\omega$ plot for finite size detector under the condition $L\omega/\sqrt{2} > 1$.

A. Density matrix for the field mode and HBAR entropy: finite size detector case

In this section we find the entropy flux corresponding to the HBAR while the finite size detector is interacting with the momentum of the field. We follow the same

procedure as described in the section (III A). For the condition $L\omega/\sqrt{2} > 1$, we find the steady state solution for the density matrix of the field as below

$$\rho_{n,n}^S = e^{-4\pi\nu n r_g/c} (1 - e^{-4\pi\nu r_g/c}). \quad (53)$$

This suggests that the rate of change of BH entropy due to photon emission in the HBAR process matches the result obtained for a point-like detector in Eq. (33). On the other hand, under the condition $L\omega/\sqrt{2} < 1$, the steady state solution is found to be $\rho^{s,s} = 0$. This implies that the commonly used approximation for the time rate of change of entropy such as

$$\dot{S}_p = -k_B \sum_{n,\nu} \dot{\rho}_{n,n} \ln \rho_{n,n} \implies \dot{S}_p \approx -k_B \sum_{n,\nu} \dot{\rho}_{n,n} \ln \rho_{n,n}^S$$

is no more valid for the case when $\rho_{n,n}^S = 0$. This hints at the possibility that under the condition $L\omega/\sqrt{2} < 1$, the system exists in a non equilibrium thermodynamic state, where standard thermal equilibrium and its consequences will no longer hold.

V. EXAMINING WIEN DISPLACEMENT FOR POINT-LIKE AND FINITE SIZE DETECTOR

In this section, we present a comparative study by examining the Wien displacement of the HBAR in the context of a point-like detector coupled minimally with the field amplitude [19] and coupling of the same with the momentum of the field. Following the same treatment as in [28] we write Eq. (17) as,

$$P(\nu)d\nu = \frac{2\pi g^2 G \nu M_{BH}}{c^3} \left(\frac{d\nu}{e^{\nu/T} - 1} \right), \quad (54)$$

where $T = \frac{\hbar c^3}{8\pi G M_{BH} k_B}$, depicts the temperature of the thermal bath due to the HBAR. Using $\hbar = k_B = c = 1$, the temperature can be recast as $T = \frac{1}{8\pi G M_{BH}}$. Using $\nu = 1/\lambda$ we write the above equation as follows,

$$P(\lambda)d\lambda = -\frac{2\pi g^2 G M_{BH}}{\lambda^3} \left(\frac{d\lambda}{e^{1/\lambda T} - 1} \right) \quad (55)$$

Upon varying with respect to the wavelength (λ) of the HBAR, the transition probability turns out to be maximum when the denominator of the Eq. (55) is minimum. Thus, writing $z = \lambda^3(e^{1/\lambda T} - 1)$, we demand,

$$\frac{dz}{d\lambda} = 0 \implies \frac{1}{3\lambda T} = 1 - e^{-1/\lambda T} \quad (56)$$

At this stage we refer our readers to the section (IV) of [28] to realise a detailed derivation of the Wien displacement in the context of HBAR phenomenon. Thus, we graphically solve this transcendental equation and obtain $\frac{1}{\lambda T} = 2.82$. Implementing the same treatment for the finite size detectors for the condition of $L\omega/\sqrt{2} > 1$,

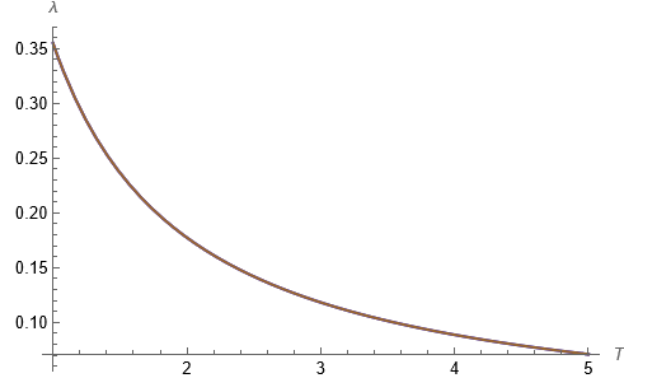


FIG. 9: Wein displacement plot with λ as a function of T . The plots corresponding to the point-like detector (in the present case), the condition $L\omega > \sqrt{2}$ and the minimally coupled model [19] coincide

we obtain the solutions for $\frac{1}{\lambda T} = 2.82$. For a clear depiction, we plot the λ vs T in the fig. (9). For $L\omega/\sqrt{2} < 1$, we are unable to perform the Wien displacement analysis due to the thermal nature of its excitation probability.

VI. DISCUSSION

Particle production in curved/ flat spacetime has been a topic of interest to many physicists since it was first proposed around 1973. Several aspects of this novel mechanism have been explored under the framework of UF effect and its applications, probing the flat/ curved spacetime using UD detector, Hawking radiation from BH, cosmological particle production, and more recently, its role in quantum entanglement, entanglement harvesting, relativistic quantum information and various new directions constantly emerging. Over the past few years, techniques from quantum optics have been extensively employed to investigate particle production, and more specifically, acceleration radiation of field quanta. This approach has resulted in several noteworthy developments such as enhancement in the temperature of the thermal bath than that of the standard UF effect, the mechanism of HBAR in curved spacetime, HBAR in the modified gravity theories such as in the context of extra dimensional BH etc. In this approach, people generally consider a single mode of the field interacting minimally with the atomic detector, that is, the detector is coupled to the field amplitude. However, literature reveals that minimally coupled atom-field interaction is affected by the IR divergences and its realistic implementation. To the best of our knowledge, this paper presents the first attempt to propose a derivative coupled atom-field interaction for investigating the HBAR phenomenon in curved spacetime. In this work, we explore the HBAR mechanism while examining both point-like and finite size atoms coupled to the momentum of the field. We obtain the transition probability of the system, where the atom undergoes a transition from

its ground state to the higher excited state and simultaneously a one-particle state of the field is generated with a particular frequency. For the point-like detector, allowing up to the leading order of perturbation theory, we find that the transition probability becomes independent of the frequency of the detector. We comment that, physically this can be viewed as the detector coupling to a field which is influenced by the local curvature of spacetime through the g^{tt} component of the metric. We hypothesise that the presence of g^{tt} modifies the sensitivity of the detector to its frequency ω , potentially expanding its effective frequency range. This condition may eliminate the sharp resonant condition that we often encounter in the context of standard HBAR process. Therefore, the transition probability becomes independent of ω up to the leading order in perturbation theory, indicating that the background geometry supplies sufficient energy to the atom-field system in order to support the transitions without requiring a sharp resonance. The outcome of this sort is entirely new in the literature of HBAR. However, the modifications in the detector's response function with respect to its frequency in the background of curved spacetime has been reported in literature in the context of UF effect and atom-mirror system [32, 37, 51]. Our results for the finite size detector suggest that the transition probability indeed depends on the extent of the detector and based on the conditions, $L\omega/\sqrt{2} > 1$ or < 1 , the probabilities show distinct behaviour while varying with respect to ν . For simplicity and for the sake of discussion, we reduce the above conditions to $L\omega \gtrsim 1$ and $L\omega \lesssim 1$ and compare the results for a fixed frequency ω . Under the condition $L\omega \gtrsim 1$, the detector's length L becomes large compared to the wavelength associated with ω . Satisfying the condition that L is also greater than the characteristic wavelength associated with ν , this implies that different parts of the detector interact with the field at different phases which leads to the destructive interference in the response of the detector. Consequently, the overall transition probability decreases. Conversely, if L is smaller with respect to the characteristics wavelength of ω in order to comply with the condition $L\omega \lesssim 1$, it spans approximately a single phase of the field which yields constructive interference in its response. In this case, if $L < \omega$, the condition L must be less than the wavelength corresponding to ν always satisfied. We refer our readers to [48, 52], where the modifications in the transition probability of the detector due to its smearing have been reported. The variation of P_{exc} with $L\omega$ for fixed field frequency, exhibits similar behaviour as described above. Furthermore, for $L\omega \lesssim 1$, we demonstrate that the steady state solution for the density matrix of the field do not exist. This signifies the breakdown of the approximation used to evaluate the time rate of change of entropy, as employed in [19]. We comment that under this condition, the system exists in a non equilibrium thermodynamic state, where the usual notions of thermal equilibrium and their consequences no longer hold.

The present work captures several new results in the context of HBAR phenomenon in curved spacetime. The interaction of the detector with the momentum of the field plays the central role to dig out these new features. In the future, investigating the enhancement of transition probabilities for point-like detectors, verifying the frequency independence of transition probabilities at the next to leading order approximation, and exploring the emergence of non equilibrium conditions for detectors of specific length could be of particular interest.

ACKNOWLEDGMENTS

AD acknowledges Soumitra Sengupta and Kinjalk Lochan for many insightful discussions and important suggestions. AK acknowledges the financial support from SRM University, AP.

APPENDIX

A. Detailed derivation of the excitation probability of the finite size detector

Following includes the intermediate steps to arrive at Eq. (37). The interaction Hamiltonian for a finite sized detector is

$$\begin{aligned} H_{int} &= \hbar g (\sigma e^{-i\omega\tau} + \sigma^\dagger e^{i\omega\tau}) \int dr' F(r') \sqrt{-g} g^{00} \partial_0 \Phi \\ &= i\hbar g \nu (\sigma e^{-i\omega\tau} + \sigma^\dagger e^{i\omega\tau}) \int dr' F(r') \frac{r^3}{r-1} \\ &\quad \left(a_\nu^\dagger e^{i\nu(t-r_*)} - a_\nu e^{-i\nu(t-r_*)} \right), \end{aligned} \quad (57)$$

where $\Phi = (a_\nu e^{-i\nu t(\tau) + i\nu r_*(\tau)} + \text{H.C.})$. Thus the excitation probability becomes,

$$\begin{aligned} P_{exc} &= \frac{1}{\hbar^2} \left| \int d\tau \langle 1, b | H_{int} | 0, a \rangle \right|^2 \\ &= \frac{g^2 \nu^2}{2\pi L^2} \left| \int_1^\infty dr \sqrt{r} e^{-\frac{2i\omega}{3} r^{3/2}} \int_1^r dr' \left(\frac{r'^3}{r'-1} \right) e^{-\frac{(r'-1)^2}{2L^2}} \right. \\ &\quad \left. e^{-i\nu(\frac{2}{3} r'^{3/2} + r' + 2 \ln(r'^{1/2} - 1) + 2r'^{1/2})} \right|^2 \end{aligned} \quad (58)$$

Substituting, $y = r^{3/2}$,

$$\begin{aligned} P_{exc} &= \frac{16g^2 \nu^2}{162\pi L^2} \left| \int_1^\infty dy e^{-\frac{2i\omega}{3} y} \int_1^y dy' \left(\frac{y'^{5/3}}{y'^{2/3} - 1} \right) \right. \\ &\quad \left. e^{-\frac{(y'^{2/3} - 1)^2}{2L^2}} e^{-i\nu(\frac{2}{3} y' + y'^{2/3} + 2y'^{1/3} + 2 \ln(y'^{1/3} - 1))} \right|^2 \end{aligned} \quad (59)$$

Further, replacing $x = \frac{2\omega}{3}(y-1)$,

$$P_{exc} = \frac{g^2 \nu^2}{2\pi L^2 \omega^4} \left| \int_0^\infty dx e^{-ix} \int_0^x dx' \frac{\left(\frac{3x'}{2\omega} + 1 \right)^{5/3}}{f(x')} \right|^2$$

$$\left| e^{-\frac{f(x')^2}{2L^2}} e^{-i\nu\Omega(x')} \right|^2 \quad (60)$$

where,

$$\begin{aligned} \Omega(x') &= \frac{2}{3} \left(\frac{3x'}{2\omega} + 1 \right) + 2 \left(\frac{3x'}{2\omega} + 1 \right)^{1/3} \\ &\quad + \left(\frac{3x'}{2\omega} + 1 \right)^{2/3} + 2 \ln \left(\left(\frac{3x'}{2\omega} + 1 \right)^{1/3} - 1 \right) \\ &= \frac{2}{3} \left(\frac{3x'}{2\omega} + 1 \right) + 2 \left(1 + \frac{1}{3} \left(\frac{3x'}{2\omega} \right) + \dots \right) + \\ &\quad \left(1 + \frac{2}{3} \left(\frac{3x'}{2\omega} \right) + \dots \right) + 2 \ln \left(1 + \frac{1}{3} \left(\frac{3x'}{2\omega} \right) + \dots - 1 \right) \end{aligned}$$

Employing the condition $1/\omega \ll 1$, we obtain,

$$\Omega(x') \approx \frac{2x'}{\omega} + 3 + 2 \ln \left(\frac{x'}{2\omega} \right) \quad (61)$$

and

$$f(x') = \left(\frac{3x'}{2\omega} + 1 \right)^{2/3} - 1 \approx \frac{x'}{\omega} \quad (62)$$

Using these approximations, the excitation probability turns out to be,

$$\begin{aligned} P_{exc} &\approx \frac{g^2 \nu^2}{2\pi L^2 \omega^4} \left| \int_0^\infty dx e^{-ix} \int_0^x dx' \frac{\omega}{x'} \left(1 + \frac{5x'}{2\omega} \right) \right. \\ &\quad \left. e^{-\frac{x'^2}{2\omega^2 L^2}} e^{-2i\nu x'/\omega} x^{-2i\nu} \right|^2 \\ &\approx \frac{g^2 \nu^2}{2\pi L^2 \omega^4} \left| \int_0^\infty dx e^{-ix} e^{-\frac{x^2}{2\omega^2 L^2}} \right. \\ &\quad \left. \int_0^x dx' \frac{\omega}{x'} \left(1 + \frac{5x'}{2\omega} \right) e^{-2i\nu x'/\omega} x^{-2i\nu} \right|^2 \quad (63) \end{aligned}$$

For the above equation, the gaussian term inside $\int dx'$ varies slowly compared to the other terms. And hence, it is taken out of the integral with $x' \rightarrow x$.

$$\begin{aligned} P_{exc} &= \frac{g^2 \nu^2}{32\pi L^2 \omega^2} \left| \int_0^\infty dx e^{-ix} e^{-x^2/2\omega^2 L^2} x^{-2i\nu} \right. \\ &\quad \left[\frac{5i}{\nu} e^{-2ix\nu/\omega} + 6\text{EI} \left(1 + 2i\nu, \frac{2i\nu x}{\omega} \right) - 6 \left(\frac{2i\nu x}{\omega} \right)^{2i\nu} \right. \\ &\quad \left. \left. \Gamma(-2i\nu) \right] \right|^2 \quad (64) \end{aligned}$$

B. Density Matrix Formulation

Following the procedure as mentioned in [23], the rate of change of the density matrix is given as, (averaged over a distribution of random injection times)

$$\dot{\rho}^P = -\kappa \int_{\tau_i}^{\tau_f} \int_{\tau_i}^{\tau'} d\tau' d\tau'' \text{Tr}_A [H(\tau'), [H(\tau''), \rho^{AP}(\tau_i)]] .$$

Here κ , is the injection rate of the atom with $\kappa = \Delta\mathcal{N}/\Delta t$. A denotes the atom and the index P stands for the field. Tracing over the atom's degrees of freedom one gets,

$$\begin{aligned} &\text{Tr}_A [H(\tau'), [H(\tau''), \rho^{AP}(\tau_i)]] \\ &= \text{Tr}_A [H' [H'', \rho^{AP}(\tau_i)] - [H'', \rho^{AP}(\tau_i)] H'] \quad (66) \end{aligned}$$

For a point-like detector, we write the Hamiltonian as below,

$$H(\tau) = g \mu(\tau) \pi(\tau) = g \frac{r^3}{r-1} \mu(\tau) \partial_0 \Phi(\tau) \quad (67)$$

We obtain $\partial_0 \Phi(\tau) = i\nu (a_\nu^\dagger e^{i\nu(t-r_*)} - \text{H.C.}) = -i\nu \varphi(\tau)$, where $\varphi(\tau) = (a_\nu^\dagger e^{i\nu(t-r_*)} - \text{H.C.}) = (a_\nu^\dagger \phi - \text{H.C.})$. Here $\phi = e^{i\nu(t-r_*)}$ [see sec. (II)]. Therefore the Hamiltonian becomes,

$$H(\tau) = ig\nu \frac{r^3}{r-1} \mu(\tau) \varphi(\tau) = ig\nu f(r) \mu(\tau) \varphi(\tau) \quad (68)$$

with $f(r) = \frac{r^3}{r-1}$. With this, the trace is,

$$\begin{aligned} &\text{Tr}_A [H' [H'', \rho^{AP}(\tau_i)] - [H'', \rho^{AP}(\tau_i)] H] \\ &= -g^2 \nu^2 \text{Tr}_A \left[f^2(r) \mu' \varphi' \mu'' \varphi'' \rho_i^{AP} - f^2(r) \mu'' \varphi'' \rho_i^{AP} \mu' \varphi' \right. \\ &\quad \left. + f^2(r) \rho_i^{AP} \mu'' \varphi'' \mu' \varphi' - f^2(r) \mu' \varphi' \rho_i^{AP} \mu'' \varphi'' \right] \\ &= -g^2 \nu^2 \left[f^2(r) \varphi' \varphi'' \rho_i^P \text{Tr}_A (\mu' \mu'' \rho_i^A) + \right. \\ &\quad \left. f^2(r) \rho_i^P \varphi'' \varphi' \text{Tr}_A (\rho_i^A \mu'' \mu') - f^2(r) \varphi' \rho_i^P \varphi'' \text{Tr}_A (\mu' \rho_i^A \mu'') - \right. \\ &\quad \left. f^2(r) \varphi'' \rho_i^P \varphi' \text{Tr}_A (\mu'' \rho_i^A \mu') \right] \\ &= -g^2 \nu^2 f^2(r) \left[\varphi' \varphi'' \rho_i^P e^{-i\omega\tau'} e^{i\omega\tau''} + \rho_i^P \varphi'' \varphi' e^{i\omega\tau'} e^{-i\omega\tau''} \right. \\ &\quad \left. - \varphi' \rho_i^P \varphi'' e^{i\omega\tau'} e^{-i\omega\tau''} - \varphi'' \rho_i^P \varphi' e^{-i\omega\tau'} e^{i\omega\tau''} \right] \quad (69) \end{aligned}$$

, where in the last step, we trace over the atom's degrees of freedom ($|a\rangle, |b\rangle$) and take the initial state of the atom's density matrix to be $|a\rangle\langle a|$. Since, $\tau' > \tau''$, the rate of change in the density matrix can be written as,

$$\begin{aligned} \dot{\rho}^P &= g^2 \nu^2 \kappa \left[\int_{\tau' > \tau''} d^2\tau f^2(r) \varphi' \varphi'' \rho^P e^{-i\omega\tau'} e^{i\omega\tau''} \right. \\ &\quad \left. + \int_{\tau' > \tau''} d^2\tau f^2(r) \rho^P \varphi'' \varphi' e^{i\omega\tau'} e^{-i\omega\tau''} - \int_{\tau' > \tau''} d^2\tau f^2(r) \right. \\ &\quad \left. \varphi' \rho^P \varphi'' e^{i\omega\tau'} e^{-i\omega\tau''} - \int_{\tau' > \tau''} d^2\tau f^2(r) \varphi'' \rho^P \varphi' e^{-i\omega\tau'} e^{i\omega\tau''} \right] . \quad (70) \end{aligned}$$

where $d\tau'd\tau'' = d^2\tau$. We can symmetrize this entire integration by swapping the region of integration of the second and the fourth terms of the above equation, that is, swapping $\tau' \leftrightarrow \tau''$ and $\varphi' \leftrightarrow \varphi''$. By naming the region $\tau' > \tau''$ as region *I* and $\tau'' > \tau'$ as region *II*, this yields,

$$\left[\varphi' \varphi'' e^{-i\omega\tau'} e^{i\omega\tau''} - \int_{I+II} d^2\tau f^2(r) \varphi' \rho^P \varphi'' e^{i\omega\tau'} e^{-i\omega\tau''} \right] \quad (71)$$

For brevity, we drop the superscript P from here on. We now find the elements of the reduced density matrix and use the notation $\rho_{nm} = \langle n | \rho | m \rangle$. We have three elements to be computed from the above expression: $\langle n | \varphi' \varphi'' \rho | n \rangle$, $\langle n | \rho \varphi' \varphi'' | n \rangle$, $\langle n | \varphi' \rho \varphi'' | n \rangle$.

$$\begin{aligned} \rho^P &= g^2 \nu^2 \kappa \left[\left(\int_I d^2\tau f^2(r) \varphi' \varphi'' \rho^P + \int_{II} d^2\tau f^2(r) \rho^P \right) \right. \\ \langle n | \varphi' \varphi'' \rho | n \rangle &= \langle n | (a_\nu^{\dagger'} \phi' - a_\nu' \phi') (a_\nu^{\dagger''} \phi'' - a_\nu'' \phi^{*''}) \rho | n \rangle \\ &= \langle n | (a_\nu^{\dagger'} \phi' a_\nu^{\dagger''} \phi'' - a_\nu^{\dagger'} \phi' a_\nu'' \phi^{*''} - a_\nu' \phi^* a_\nu^{\dagger''} \phi'' + a_\nu' \phi^* a_\nu'' \phi^{*''}) \rho | n \rangle \\ &= \phi' \phi'' \langle n | a_\nu^{\dagger'} a_\nu^{\dagger''} \rho | n \rangle - \phi' \phi^{*''} \langle n | a_\nu^{\dagger'} a_\nu'' \rho | n \rangle - \phi^{*'} \phi'' \langle n | a_\nu' a_\nu^{\dagger''} \rho | n \rangle + \phi^{*'} \phi^{*''} \langle n | a_\nu' a_\nu'' \rho | n \rangle \\ &= \sqrt{n(n-1)} \phi' \phi'' \langle n-2 | \rho | n \rangle - n \phi' \phi^{*''} \langle n | \rho | n \rangle - \\ &\quad (n+1) \phi^{*'} \phi'' \langle n | \rho | n \rangle + \sqrt{(n+1)(n+2)} \phi^{*'} \phi^{*''} \langle n+2 | \rho | n \rangle \\ &= \sqrt{n(n-1)} \phi' \phi'' \rho_{n-2,n} - n \phi' \phi^{*''} \rho_{n,n} - (n+1) \phi^{*'} \phi'' \rho_{n,n} + \sqrt{(n+1)(n+2)} \phi^{*'} \phi^{*''} \rho_{n+2,n} \end{aligned} \quad (72)$$

Similarly, we get

$$\langle n | \rho \varphi' \varphi'' | n \rangle = \sqrt{(n+1)(n+2)} \phi' \phi'' \rho_{n,n+2} - n \phi' \phi^{*''} \rho_{n,n} - (n+1) \phi^{*'} \phi'' \rho_{n,n} + \sqrt{n(n-1)} \phi^{*'} \phi^{*''} \rho_{n,n-2} \quad (73)$$

$$\langle n | \varphi' \rho \varphi'' | n \rangle = \sqrt{n(n+1)} \phi' \phi'' \rho_{n-1,n+1} - n \phi' \phi^{*''} \rho_{n-1,n-1} - (n+1) \phi^{*'} \phi'' \rho_{n+1,n+1} + \sqrt{n(n+1)} \phi^{*'} \phi^{*''} \rho_{n+1,n-1} \quad (74)$$

As the injection time is random, we consider only the diagonal elements of the matrix where for $\rho_{m,n}$, $m = n$. The first two terms of (71)

$$\begin{aligned} &\langle n | \left(\int_I d^2\tau f^2(r) \varphi' \varphi'' \rho^P + \int_{II} d^2\tau f^2(r) \rho^P \varphi' \varphi'' \right) e^{-i\omega\tau'} e^{i\omega\tau''} | n \rangle \\ &= e^{-i\omega\tau'} e^{i\omega\tau''} \left(- \int_{I+II} d^2\tau f^2(r) n \phi' \phi^{*''} \rho_{n,n} + (n+1) \phi^{*'} \phi'' \rho_{n,n} \right) \\ &= - \left(\int_{\tau_i}^{\tau_f} d\tau' f(r) \phi' e^{-i\omega\tau'} \int_{\tau_i}^{\tau_f} d\tau'' f(r) \phi^{*''} e^{i\omega\tau''} \right) n \rho_{n,n} - \left(\int_{\tau_i}^{\tau_f} d\tau' f(r) \phi^{*'} e^{-i\omega\tau'} \int_{\tau_i}^{\tau_f} d\tau'' f(r) \phi'' e^{i\omega\tau''} \right) (n+1) n \rho_{n,n} \\ &= -|I_{a,s}|^2 n \rho_{n,n} - |I_{e,s}|^2 (n+1) n \rho_{n,n}, \end{aligned} \quad (75)$$

where $|I_{e,s}|^2 = \left| \int d\tau f(r) \psi e^{i\omega\tau} \right|^2$ and $|I_{a,s}|^2 = \left| \int d\tau f(r) \psi e^{-i\omega\tau} \right|^2$. Similarly, we get third and the fourth terms as,

$$\begin{aligned} &\langle n | \int_{I+II} d^2\tau f^2(r) \varphi' \rho^P \varphi'' e^{i\omega\tau'} e^{-i\omega\tau''} | n \rangle = \int_{I+II} d^2\tau f^2(r) (-n \phi' \phi^{*''} \rho_{n-1,n-1} - (n+1) \phi^{*'} \phi'' \rho_{n+1,n+1}) e^{i\omega\tau'} e^{-i\omega\tau''} \\ &= -|I_{e,s}|^2 n \rho_{n-1,n-1} - |I_{a,s}|^2 (n+1) \rho_{n+1,n+1} \end{aligned} \quad (76)$$

Therefore the reduced density matrix is now,

$$\begin{aligned} &= -R_e((n+1)\rho_{n,n} - n\rho_{n-1,n-1}) \\ &\quad - R_a(n\rho_{n,n} - (n+1)\rho_{n+1,n+1}) \end{aligned} \quad (77)$$

$$\begin{aligned} \rho^P &= g^2 \nu^2 \kappa \left[-|I_{a,s}|^2 n \rho_{n,n} - |I_{e,s}|^2 (n+1) n \rho_{n,n} \right. \\ &\quad \left. + |I_{e,s}|^2 n \rho_{n-1,n-1} + |I_{a,s}|^2 (n+1) \rho_{n+1,n+1} \right] \\ &= -\kappa P_{exc}((n+1)\rho_{n,n} - n\rho_{n-1,n-1}) \\ &\quad - \kappa P_{abs}(n\rho_{n,n} - (n+1)\rho_{n+1,n+1}) \end{aligned}$$

where $P_{exc/abs} = g^2 \nu^2 |I_{e,s/a,s}|^2$, and R_e and R_a are the emission rate and the absorption rate respectively, with $R_{e/a} = \kappa P_{exc/abs}$. The steady state solution of the density matrix will thus be,

$$\rho_{n,n}^S = C \left(\frac{R_e}{R_a} \right)^n \quad (78)$$

where C is a normalization constant that can be evaluated using the Trace property of a density matrix.

$$\text{Tr} \rho_{n,n}^S = \sum_{n=0}^{\infty} \rho_{n,n}^S = C \sum_{n=0}^{\infty} \left(\frac{R_e}{R_a} \right)^n = 1 \quad (79)$$

For a point like detector,

$$\begin{aligned} \rho_{n,n}^S &= C \left(\frac{R_e}{R_a} \right)^n = C \left(\frac{P_{exc}}{P_{abs}} \right)^n = C e^{-4\pi\nu n r_g/c} \\ \text{Tr} \rho_{n,n}^S &= \sum_{n=0}^{\infty} \rho_{n,n}^S \\ &= C \sum_{n=0}^{\infty} e^{-4\pi\nu n r_g/c} = C \left(\frac{1}{1 - e^{-4\pi\nu r_g/c}} \right) = 1 \end{aligned}$$

$$\therefore \rho_{n,n}^S = (1 - e^{-4\pi\nu r_g/c}) e^{-4\pi\nu n r_g/c} \quad (80)$$

For the finite-sized detector, with the Hamiltonian $H_{int} = g\mu(\tau) \int dr' F(r') \sqrt{-g}^{00} \partial_0 \phi$, we get the same form for steady state solution of the reduced density matrix as (78) when we follow the same steps. For the case (where $L\omega > \sqrt{2}$), we get

$$P_{abs} = e^{-4\pi\nu r_g/c} P_{exc} \quad (81)$$

Hence, the steady state solution of density matrix is

$$\rho_{n,n}^S = C \left(\frac{R_e}{R_a} \right)^n = (1 - e^{-4\pi\nu r_g/c}) e^{-4\pi\nu n r_g/c} \quad (82)$$

which is same as that of the point-like detector. However, in case of $L\omega < \sqrt{2}$, $P_{e,s} = P_{a,s}$, and thus $C = 0$ implying $\rho_{n,n}^S = 0$

-
- [1] S. W. Hawking, “Particle Creation by Black Holes,” *Commun. Math. Phys.* **43**, 199-220 (1975) [erratum: *Commun. Math. Phys.* **46**, 206 (1976)]
 - [2] S. W. Hawking, “Black Holes and Thermodynamics,” *Phys. Rev. D* **13**, 191-197 (1976)
 - [3] L. Parker, “Quantized fields and particle creation in expanding universes. 1.,” *Phys. Rev.* **183**, 1057-1068 (1969).
 - [4] L. Parker, “Particle creation in expanding universes,” *Phys. Rev. Lett.* **21**, 562-564 (1968).
 - [5] L. Parker, “Quantized fields and particle creation in expanding universes. 2.,” *Phys. Rev. D* **3**, 346-356 (1971) *Phys. Rev. D* **3**, 2546-2546 (1971).
 - [6] W. G. Unruh, “Origin of the Particles in Black Hole Evaporation,” *Phys. Rev. D* **15**, 365-369 (1977).
 - [7] G. W. Gibbons and S. W. Hawking, “Cosmological Event Horizons, Thermodynamics, and Particle Creation,” *Phys. Rev. D* **15**, 2738-2751 (1977).
 - [8] S. J. Summers and R. Werner, “The vacuum violates Bell’s inequalities,” *Phys. Lett. A* **110**, no.5, 257-259 (1985).
 - [9] I. Fuentes-Schuller and R. B. Mann, ‘Alice falls into a black hole: Entanglement in non-inertial frames,” *Phys. Rev. Lett.* **95**, 120404 (2005)
 - [10] S. J. Summers and R. Werner, “Maximal Violation of Bell’s Inequalities Is Generic in Quantum Field Theory,” *Commun. Math. Phys.* **110**, 247-259 (1987)
 - [11] A. Pozas-Kerstjens and E. Martin-Martinez, “Harvesting correlations from the quantum vacuum,” *Phys. Rev. D* **92**, no.6, 064042 (2015).
 - [12] B. Reznik, “Entanglement from the vacuum,” *Found. Phys.* **33**, 167-176 (2003).
 - [13] T. C. Ralph and R. B. Mann, “Relativistic quantum information,” *Class. Quant. Grav.* **29**, no.22, 220301 (2012).
 - [14] E. Martin-Martinez, “Relativistic Quantum Information: developments in Quantum Information in general relativistic scenarios,” *Ph.D. thesis, Waterloo U.*, (2011).
 - [15] M. O. Scully, V. V. Kocharovsky, A. Belyanin, E. Fry and F. Capasso, “Enhancing Acceleration Radiation from Ground-State Atoms via Cavity Quantum Electrodynamics,” *Phys. Rev. Lett.* **91**, 243004 (2003).
 - [16] W. G. Unruh, “Notes on black hole evaporation,” *Phys. Rev. D* **14**, 870 (1976)
 - [17] N. D. Birrell and P. C. W. Davies, “Quantum Fields in Curved Space,” *Cambridge University Press*, 1982, ISBN 978-0-511-62263-2, 978-0-521-27858-4
 - [18] L. C. B. Crispino, A. Higuchi and G. E. A. Matsas, “The Unruh effect and its applications,” *Rev. Mod. Phys.* **80**, 787-838 (2008).
 - [19] M. O. Scully, S. Fulling, D. Lee, D. N. Page, W. Schleich and A. Svidzinsky, “Quantum optics approach to radiation from atoms falling into a black hole,” *Proc. Nat. Acad. Sci.* **115**, no.32, 8131-8136 (2018).
 - [20] A. A. Svidzinsky, J. S. Ben-Benjamin, S. A. Fulling and D. N. Page, “Excitation of an Atom by a Uniformly Accelerated Mirror through Virtual Transitions,” *Phys. Rev. Lett.* **121**, no.7, 071301 (2018)
 - [21] H. E. Camblong, A. Chakraborty and C. R. Ordonez, “Near-horizon aspects of acceleration radiation by free fall of an atom into a black hole,” *Phys. Rev. D* **102**, no.8, 085010 (2020).
 - [22] A. Azizi, H. E. Camblong, A. Chakraborty, C. R. Ordonez and M. O. Scully, “Acceleration radiation of an atom freely falling into a Kerr black hole and near-horizon conformal quantum mechanics,” *Phys. Rev. D* **104**, no.6, 065006 (2021).
 - [23] A. Azizi, H. E. Camblong, A. Chakraborty, C. R. Ordonez and M. O. Scully, “Quantum optics meets black hole thermodynamics via conformal quantum mechanics: I. Master equation for acceleration radiation,” *Phys. Rev. D* **104**, 084086 (2021).
 - [24] A. Azizi, H. E. Camblong, A. Chakraborty, C. R. Ordonez and M. O. Scully, “Quantum optics meets black hole thermodynamics via conformal quantum mechanics: II. Thermodynamics of acceleration radiation,” *Phys. Rev. D* **104**, 084085 (2021).
 - [25] S. Sen, R. Mandal and S. Gangopadhyay, “Equivalence principle and HBAR entropy of an atom falling into a quantum corrected black hole,” *Phys. Rev. D* **105**, no.8, 085007 (2022).
 - [26] S. Sen, R. Mandal and S. Gangopadhyay, “Near horizon

- aspects of acceleration radiation of an atom falling into a class of static spherically symmetric black hole geometries,” *Phys. Rev. D* **106**, no.2, 025004 (2022).
- [27] A. Das, S. Sen and S. Gangopadhyay, “Virtual transitions in an atom-mirror system in the presence of two scalar photons,” *Phys. Rev. D* **107**, no.2, 025009 (2023).
- [28] A. Das, S. Sen and S. Gangopadhyay, “Horizon brightened accelerated radiation in the background of braneworld black holes,” *Phys. Rev. D* **109**, no.6, 064087 (2024).
- [29] S. Takagi, “Vacuum Noise and Stress Induced by Uniform Acceleration: Hawking-Unruh Effect in Rindler Manifold of Arbitrary Dimension,” *Prog. Theor. Phys. Suppl.* **88**, 1-142 (1986).
- [30] B. A. Juárez-Aubry and J. Louko, “Quantum kicks near a Cauchy horizon,” *AVS Quantum Sci.* **4**, no.1, 013201 (2023).
- [31] C. R. D. Bunney and J. Louko, “Circular motion analogue Unruh effect in a thermal bath: robbing from the rich and giving to the poor,” *Class. Quant. Grav.* **40**, no.15, 155001 (2023).
- [32] B. A. Juárez-Aubry and J. Louko, “Onset and decay of the $1 + 1$ Hawking-Unruh effect: what the derivative-coupling detector saw,” *Class. Quant. Grav.* **31**, no.24, 245007 (2014).
- [33] E. Martín-Martínez and J. Louko, “Particle detectors and the zero mode of a quantum field,” *Phys. Rev. D* **90**, no.2, 024015 (2014).
- [34] A. Raval, B. L. Hu and J. Anglin, “Stochastic theory of accelerated detectors in a quantum field,” *Phys. Rev. D* **53**, 7003-7019 (1996).
- [35] Q. Wang and W. G. Unruh, “Motion of a mirror under infinitely fluctuating quantum vacuum stress,” *Phys. Rev. D* **89**, no.8, 085009 (2014).
- [36] E. Tjoa and R. B. Mann, “Harvesting correlations in Schwarzschild and collapsing shell spacetimes,” *JHEP* **08**, 155 (2020).
- [37] J. Louko, “Unruh-DeWitt detector response across a Rindler firewall is finite,” *JHEP* **09**, 142 (2014).
- [38] A. Teixidó-Bonfill and E. Martín-Martínez, “Derivative coupling enables genuine entanglement harvesting in causal communication,” *Phys. Rev. D* **110**, no.10, 105016 (2024).
- [39] B. A. Juárez-Aubry and J. Louko, “Quantum fields during black hole formation: How good an approximation is the Unruh state?,” *JHEP* **05**, 140 (2018).
- [40] T. R. Perche and M. H. Zambianco, “Duality between amplitude and derivative coupled particle detectors in the limit of large energy gaps,” *Phys. Rev. D* **108**, no.4, 045017 (2023).
- [41] M. Kasprzak and E. Tjoa, “Transmission of quantum information through quantum fields in curved spacetimes,” *J. Phys. A* **58**, no.9, 095301 (2025).
- [42] A. Pozas-Kerstjens and E. Martín-Martínez, “Entanglement harvesting from the electromagnetic vacuum with hydrogenlike atoms,” *Phys. Rev. D* **94**, no.6, 064074 (2016).
- [43] R. Lopp and E. Martín-Martínez, “Quantum delocalization, gauge, and quantum optics: Light-matter interaction in relativistic quantum information,” *Phys. Rev. A* **103**, no.1, 013703 (2021).
- [44] E. McKay, A. Lupascu and E. Martín-Martínez, “Finite sizes and smooth cutoffs in superconducting circuits,” *Phys. Rev. A* **96**, no.5, 052325 (2017).
- [45] N. Janzen, X. Dai, S. Ren, J. Shi and A. Lupascu, “Tunable coupler for mediating interactions between a two-level system and a waveguide from a decoupled state to the ultrastrong coupling regime,” *Phys. Rev. Res.* **5**, no.3, 033155 (2023).
- [46] S. Schlicht, “Considerations on the Unruh effect: Causality and regularization,” *Class. Quant. Grav.* **21**, 4647-4660 (2004).
- [47] P. Langlois, “Causal particle detectors and topology,” *Annals Phys.* **321**, 2027-2070 (2006).
- [48] J. Louko and A. Satz, “How often does the Unruh-DeWitt detector click? Regularisation by a spatial profile,” *Class. Quant. Grav.* **23**, 6321-6344 (2006).
- [49] E. Martín-Martínez, M. Montero and M. del Rey, “Wavepacket detection with the Unruh-DeWitt model,” *Phys. Rev. D* **87**, no.6, 064038 (2013).
- [50] J. Louko and A. Satz, “Excited by a quantum field: Does shape matter?,” *J. Phys. Conf. Ser.* **68**, 012014 (2007).
- [51] J. Louko and A. Satz, “Transition rate of the Unruh-DeWitt detector in curved spacetime,” *Class. Quant. Grav.* **25**, 055012 (2008).
- [52] A. R. Lee and I. Fuentes, “Spatially extended Unruh-DeWitt detectors for relativistic quantum information,” *Phys. Rev. D* **89**, no.8, 085041 (2014).